28. Radio-Frequency Sounders in Space

S. A. Pulinets[1] and R. F. Benson[2]

[1]Institute of Terrestrial Magnetism, Ionosphere and Radiowave Propagation
IZMIRAN, Troitsk, Moscow Region, 142092 Russia
Tel: +7 095 334 0919; Fax: +7 095 334 0124; E-mail: pulse@izmiran.rssi.ru

[2]Laboratory for Extraterrestrial Physics
Code 692, NASA Goddard Space Flight Center
Greenbelt, MD 20771, USA
Tel: +1 (301) 286-4037; Fax: +1 (301) 286-1683
E-mail: u2rfb@lepvax.gsfc.nasa.gov

1. Abstract

Radio-frequency sounders in space are most often referred to as topside sounders, because their original purpose was to investigate the global distribution of electron density in the ionosphere at altitudes above the F-layer peak density. They have been used predominantly for four types of investigations: (1) local and remote topside electron densities and electron-density gradients, (2) wave propagation, (3) natural emissions, and (4) stimulated plasma emissions. This paper will give a brief overview of recent results that have been obtained in these areas from investigations of ionograms from the Alouette/ISIS (International Satellites for Ionospheric Studies), Interkosmos-19/Cosmos 1809, and other topside-sounder programs, and will discuss perspectives of future investigations using radio-frequency sounders in space.

2. Introduction

Topside sounders made a revolutionary contribution to our knowledge of the Earth's ionosphere and space plasma physics. They changed our view from a single overhead look to a global coverage of the near-Earth space. Information about the large-scale global structure and dynamics of the ionosphere was realized. The equatorial anomaly, main trough, and other irregularities appeared in all their complexity and non-predictability. The methods of ionogram reduction into vertical profiles of electron concentration were developed and improved. The topside sounders opened up the possibility of having total profiles of electron concentration,

not only in selected locations near ground-based radars and ionosondes, but also globally.

In the euphoria of the first successes of empirical-data collection and the progress of theoretical modeling of the ionosphere, however, it was practically a common decision that our knowledge of the ionosphere was close to comprehensive, and that it would not be necessary to continue launching such complex devices as satellite ionospheric sounders. Many physicists shifted their attention to magnetospheric and planetary sciences, wave and particle measurements became more popular, and topside sounders moved to the margin of ionospheric studies. For more than 10 years, there were no topside sounders in orbit, regular studies were stopped, and it looked as if this technique was forgotten.

As it has now become clear, this pause was mainly due to the difficulties of systematic production of topside ionograms, and the routine conversion of ionogram traces to electron-concentration profiles. In addition, the potential scientific output from topside sounders was underestimated. This new understanding has been gained during the course of topside-sounder data processing that revealed new features of the global structure of the ionosphere, as well as new fields of topside-sounder application. The present paper will mainly be devoted to these two topics.

2.1. History

Those interested in the history of topside sounders can find detailed information in a special issue of the *Proceedings of the IEEE* [*IEEE, 1969*] and in [*Pulinets, 1989*]. We will discuss only the main milestones here. The name "topside sounder" formally can be given to more than ten satellite-borne instruments launched by different countries: Alouette I (1962), Explorer 20 (1964), Alouette II (1965), ISIS I (1969), Cosmos-381 (1970), ISIS II (1971), ISS-A (1976), ISS-B (1978), EXOS-B (1978), ISEE 1 and 2 (1978), Interkosmos-19 (1979), EXOS-C (1984), Cosmos 1809 (1986), EXOS-D (1989), CORONAS-I (1994). These can, in fact, be divided into several groups according to inherent ideas and parameters. Every instrument had its own merit, but we can divide the topside-sounder era into three periods:

1. First discoveries of the large-scale global structure of the ionosphere and the physics of plasma resonances (Alouette and ISIS).

2. First global mapping of the topside ionosphere (ISS-B).

3. Fundamental study of the global ionospheric structure and dynamics, and practical applications of the results (Interkosmos-19 and Cosmos 1809).

An effort is underway to transform selected samples of several decades of ISIS-I and -II ionospheric topside-sounder data to digital ionograms [*Benson, 1996*].

The digital ionograms are available via the World Wide Web at the following URL: http://nssdc.gsfc.nasa.gov/space/isis/isis-status.html . A proposal has been drafted by one of the authors (SP) to make the Interkosmos-19/Cosmos 1809 ionograms at the Institute of Terrestrial Magnetism, Ionosphere and Radiowave Propagation, Russian Academy of Sciences (IZMIRAN) at Troitsk available in a similar manner.

The next period will be opened by magnetospheric radio sounding [*Calvert et al., 1995*] and advanced topside-sounder missions with Doppler and direction-finding capabilities [*Reinisch, 1998*], at the start of the third millennium.

2.2. Sounding principles–wave propagation

The main difference between topside and bottom-side sounding is that the transmitting and receiving antennas of the topside sounder are immersed in the ionospheric plasma, so the interaction of the emitted wave with the plasma starts immediately in the vicinity of the satellite. According to the wave-dispersion relation for a magnetized plasma, electromagnetic waves of different polarizations can propagate in a plasma only at frequencies higher than the so-called cut-off frequencies, which are

$$f_Z = \frac{\sqrt{4f_N^2 + f_H^2}}{2} - \frac{f_H}{2}$$ left-hand-polarized slow extraordinary mode

f_N (local electron plasma frequency): left-hand-polarized fast ordinary mode

$$f_X = \frac{\sqrt{4f_N^2 + f_H^2}}{2} + \frac{f_H}{2}$$ right-hand-polarized fast extraordinary mode

The group velocities of the waves near the cutoff frequencies are very low. As frequency increases above the cutoff, the group velocity increases, approaching the propagation velocity of electromagnetic waves in a vacuum.

As the reflection point is approached, with increasing electron density below the satellite, the group velocity decreases to zero and changes sign. On topside ionograms, the total echo group delay at each frequency to this point of reflection is converted to an "apparent range" by dividing by two and then multiplying by the free-space light velocity. An ISIS-II digital ionogram is shown in Figure 1. The horizontal line at 11.11 ms echo-delay time is a calibration marker, corresponding to 1667 km apparent range. In order to obtain the real electron-density profile, it is necessary to solve the problem of the group path $p'(f)$ integral [*Jackson, 1969*]. During the last few years, the Jackson algorithm was improved by *Denisenko et al.* [*1998 a,b,c*] with the use of the regularization technique. In addition, they proposed

an algorithm to calculate the bottom-side profiles from the ground reflection trace on topside ionograms.

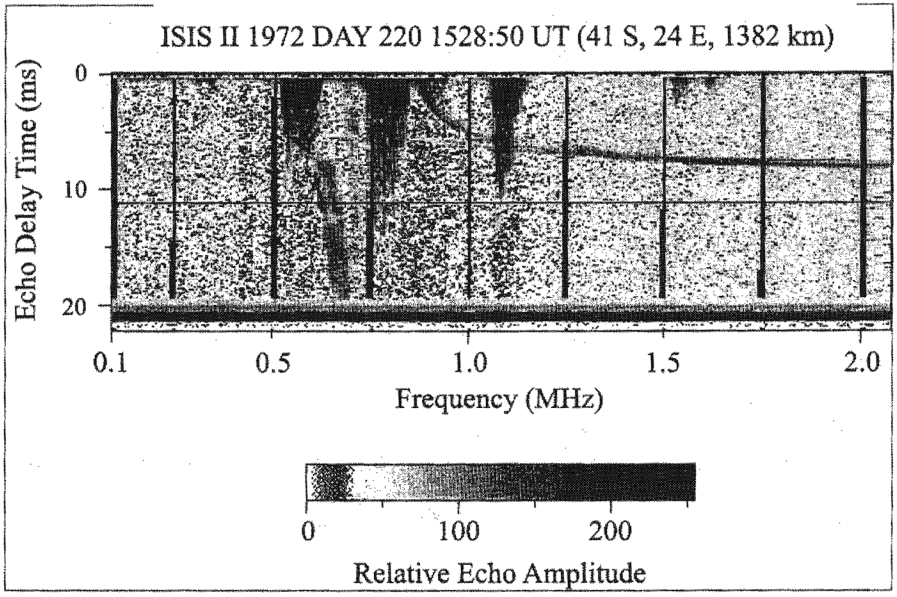

Figure 1. A portion of a digital ISIS-II ionogram recorded at Johannesburg. Only the 0.1-2.0 MHz portion of the 0.1-20 MHz ionogram is reproduced above. Z, O, and X-wave reflection traces are observed (Z, on the left, and X up to zero delay time) in addition to plasma resonances, including those at the electron gyrofrequency and the electron plasma frequency (just to the right of the 0.5 MHz marker), the upper-hybrid frequency (just to the right of the 0.75 MHz marker), and the second harmonic of the electron gyrofrequency (to the right of the 1.0 MHz marker). The satellite location corresponded to 1706 magnetic local time and -51° invariant latitude.

In principle, all calculations assume vertical wave propagation and a horizontally stratified medium. Based on this assumption, only vertically reflected rays will return to the satellite. In practice, however, due to the presence of plasma irregularities and plasma gradients, the orthogonal-reflection condition can be fulfilled for any direction. These conditions sometimes lead to additional reflections and traces on topside ionograms, especially in high latitudes and the equatorial regions. Small-scale irregularities cause wave scattering, which is strongest in the Z-mode frequency domain. The intensity of the scattered signal can be used for the global monitoring of small-scale plasma irregularities [*Zabotin et al., 1997*].

2.3 Sounding principles–instrument parameters

We should be more precise when using the words "sounding" and "topside sounder." Some of the instruments mentioned above should only be considered "relaxation sounders." Their pulsed HF emissions only excite the near-satellite plasma in the form of plasma resonances. Sometimes they are able to receive the reflections from the lower layers of the ionosphere, or from irregularities, but they are not able to receive the complete topside-ionogram trace necessary to obtain the vertical profile of electron concentration. From this point of view we should limit a list of sounders to Alouette I and II, ISIS I and II, ISS-B, Interkosmos-19, Cosmos 1809, and Coronas-I.

There are several parameters that are crucial for topside sounding.

2.3.1 Orbit height. For classical sounding, the satellite orbit should be high enough to detect the transition height between the dominant ionized constituents O^+ and He^+ ions, which is usually near 750 km. From another point of view, a higher orbit (> 1200 km) leads to wave trapping in magnetic-field-aligned electron-density irregularities in high-latitude regions, i.e., to non-vertical ray propagation. It is now accepted that an optimal orbit for topside sounding is circular polar from 800 to 1000 km height. Nevertheless, recent papers have considered the possibility of sounding from low-orbiting platforms, such as the Russian "Mir" space station or the future International Space Station [*Danilkin and Vaisman, 1997*; *Danilkin et al., 1998*]. This technique uses ground-reflection traces, as well as multiple reflections from the ground and upper layers (up to eight different traces). Naturally, this technique will only yield information about the bottom-side ionosphere. However, it will be global, with a uniform space distribution, in contrast to the irregular coverage provided by the network of ground-based ionospheric stations.

2.3.2 Ionogram duration. One should keep in mind that topside sounding is conducted from a moving object with a speed of approximately 7 km/s. At the same time, the sounding process sweeps the frequency domain from ~ 0.1 up to 16-20 MHz. In order to receive the signal reflected from the ionosphere, the sounder receiver should remain tuned to each frequency for no less than 15-20 ms. Therefore, the ionogram duration could be (depending on the number of frequency steps) from 5 s (CORONAS-I) to 32 s (Alouette II). To study the ionospheric structures with large density gradients–such as the main ionospheric trough, where the electron density can change by an order of magnitude over a distance of 300-500 km–a short-duration ionogram, interpreted as a one-point measurement, is very important.

2.3.3 Sounding pulse duration. As in bottom-side sounding, the pulse duration determines the height resolution of the topside sounder. Here, a compromise should be reached between high resolution and the energy contained in the transmitted pulse. Usually the pulse duration for topside sounders lies within the interval of 80-100 μs. To increase the resolution, while not sacrificing the

transmitted pulse energy, as well as for Doppler and phase measurements, pulse coding has been proposed [*Reinisch, 1996*], with pulse durations as short as 33 μs.

2.3.4 Emitted power. It was shown by Interkosmos-19 and Cosmos 1809 wave and particle measurements, and then supported by ISIS results, that the near-satellite plasma is strongly modified by topside-sounder transmitter pulses [*Baranets et al., 1995*]. In the case of Interkosmos-19 and ISIS, the emitted power was 300-500 W. The advanced design, including pulse-coding and antenna-matching techniques, used in the proposed TOPside Automated Doppler Sounder (TOPADS) instrument for the Warning mission (see http://space.ups.kiev.ua/projects/warning/) permit reductions in the emitted power to 10 W.

2.3.5 Frequency and height resolution. These parameters determine the quality of the information obtained in at least two domains:

- The precision of determining the cutoff frequencies f_Z, f_N, and f_X, the critical frequencies $f_0\,\mathrm{F2}$ and $f_X\,\mathrm{F2}$ in the frequency bands where steep gradients of group velocity with frequency and height are observed;

- The precision of determining the frequencies of plasma resonances.

3. Global ionospheric structure and dynamics

The ionospheric models presently used are constructed mainly from data from ground ionospheric stations. Since they are located non-uniformly on the globe, a lot of spatial areas, as well as ionospheric parameters, are covered inadequately. Topside-sounding data allow these blanks to be filled in, and will reveal previously unknown features of the electron concentration (N_e) distribution in the ionosphere. The main advantage of the Interkosmos-19 satellite, compared with all other topside sounders launched to date, was the large onboard memory that permitted continuous sounding of the ionosphere for up to 17 hours (10 orbits), in order to produce three-dimensional distributions of N_e without longitude restrictions. Interkosmos-19 was active from 1979-81, i.e., during high solar activity. The inclination of its orbit was 74°, so it crossed middle and low latitudes in an almost meridional direction, with a longitude interval of 25° between orbits. The local time of this crossing changed very slowly, by approximately one hour in five days.

3.1. Global longitudinal effect and main trough

One of the main features of the global structure of the ionosphere revealed by Interkosmos-19 was the strong and steady longitudinal effect that was observed at all latitudes [*Karpachev, 1995,1996*]. The variations of the F2-layer maximum parameters with longitude for night-time summer conditions at an invariant latitude

of 40° (in both hemispheres) was investigated. It was shown that the longitudinal effect at middle latitudes has a steady character in N_mF2 and T_e, and a less stable one in h_mF2. These parameters are the density at the peak of the F2 layer, the electron temperature, and the height of the F2 peak, respectively. The new version of the IRI model (IRI-95) reproduces the longitudinal variations in N_mF2 very well, but is much worse in h_mF2, and is completely inadequate in reproducing the observed longitudinal variations in T_e. The calculations of the vertical drift from h_mF2 values, by means of the model developed in IZMIRAN [*Karpachev and Gasilov, 1998*], showed that the longitudinal variations in N_mF2 and h_mF2 are caused, mainly, by the neutral-wind effect and, partially, by the longitudinal variations of thermospheric parameters. The Horizontal Wind Model-93 neutral-wind model [*Hedin et al., 1996*] inadequately reproduces the vertical-drift variations for the above-mentioned conditions.

One of the striking features revealed in the Interkosmos-19 data was the strong asymmetry between hemispheres in the configuration of the summer trough. This is illustrated in Figure 2, where data for local summers are presented (June for the northern hemisphere and December for southern hemisphere). The asymmetry basically results from the effect of the zonal wind component due to variations of the magnetic-field declination with longitude, and with changes of the meridional wind magnitude with geographical latitude. The longitudinal variations of the neutral atmospheric parameters, which are very different in each hemisphere, are of some importance, too. The trough can be observed in summer nighttime conditions in areas of full shadow and minimal background concentration, which occur from 210°-270° E in the northern hemisphere. The ripple or "cliff" of ionization, brightly appearing as the maximum density at latitudes 50°-60° and longitudes 240°-300° in the southern hemisphere, is observed at longitudes 120°-150° in the northern hemisphere in a less-expressed character. Thus, the trough can be observed on summer nights in quiet conditions over North America, but not over Europe.

As a result of many years of Interkosmos-19 satellite data analysis, a new model of the mid-latitude ionospheric trough was developed, based on data from the Interkosmos-19 and Cosmos-900 satellites (over 1500 orbits) [*Karpachev et al., 1996*]. It is valid for nighttime (18 to 06 MLT), winter and equinox, and Kp-indices from 0 to 8. It covers the topside ionosphere up to 1000 km, and describes the trough minimum position depending on longitude, altitude, magnetic local time (MLT), and Kp-index. The model is presented in analytical form, as well as a nomogram versus MLT and Kp, and a nighttime segment of a circle (in polar coordinates) with the radius as a function of the Kp-index. The effective Kp-index, taken for the preceding 4.4 hours, is used in the model.

In addition to the main ionospheric trough (MIT), the ring ionospheric trough (RIT) was extracted and studied. Contrary to the main ionospheric trough, the RIT correlates poorly with the Kp-index. It is observed only during the storm recovery

phase at invariant latitudes near 55°, and is connected to a residual ring magnetospheric current and to steady red auroral arcs (SAR-arcs).

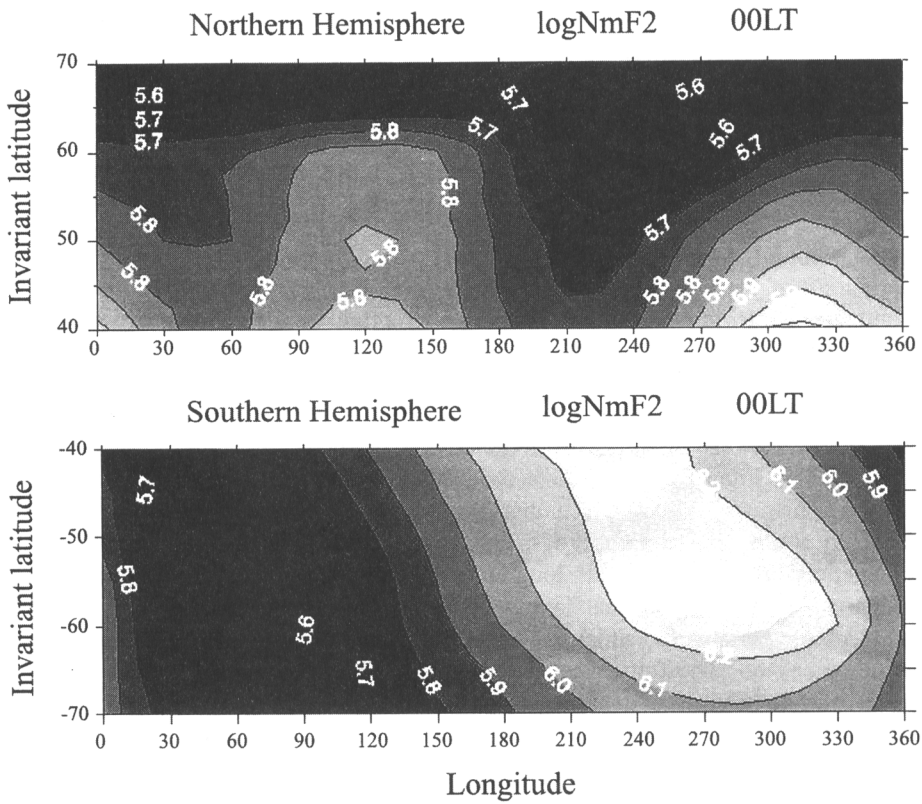

Figure 2. The global (all longitudes) peak electron-density distribution in the vicinity of the main trough for local summer nighttime conditions (high solar activity), from the Interkosmos-19 topside-sounding data: (upper panel) northern hemisphere, (lower panel) southern hemisphere.

3.2. Equatorial anomaly

In the vicinity of the equatorial anomaly, the longitudinal effect has a more complex character. In the majority of cases (more than 80%), the longitudinal variations have a regular wavy character, with a period of about 75° in longitude.

The average amplitude of this feature is 2-3 MHz on the dip equator and 3-4 MHz on the crests of the Appleton anomaly [*Deminova, 1995a*]. The longitudinal variations of $f_0 F2$ on the crests of the anomaly are usually in opposite phase, relative to those along the dip equator. On the average, the extrema of these wave

structures settle down on the same longitudes. The changes of the average longitudinal position of these extrema during nighttime (21-05 LT) and from season to season were not prominent. Along the dip equator, the minima of f_0F2 were observed, on average, to be at longitudes close to 45°, 130°, 200°, and 330°. The minimum close to 330° is the deepest, and is especially prominent during the June solar-solstice. At the transition from the crests of the anomaly to the average latitudes, such wavy structure gradually disappears, and at invariant latitudes above 30° it practically does not exist.

3.3. Disturbed conditions

Topside sounding from a satellite reveals how the ionosphere reacts to geomagnetic storms on a global scale. A schematic pattern of a global ionospheric response to a magnetic disturbance was constructed using the strong storm of April 3-4, 1979, as an example for further study [*Karpachev et al., 1995*]. It was shown that the nightside winter trough position during the storm growth phase correlated best with K_p index, at a time delay proportional to a disturbance growth rate $d\,\mathrm{Kp}/dt$. The dependence of the MIT location on D_{st}, B_Z, and B_Y was also shown. Two troughs were found to be formed, usually during the storm recovery phase at post-midnight hours: the MIT and the RIT, associated with the DR-current. In general, the response of the MIT position to a southward turning of B_Z corresponds well to the equatorial edge dynamics of auroral diffuse precipitation. Under isolated B_Z southward turnings, the height of the equatorial night-time F layer decreases by 50-100 km, and when B_Z turns northward, the low latitude F layer rises. The latter effect is most pronounced at 03 LT [*Deminova, 1995b*]. Such vertical movements of ionospheric plasma occur under the action of an additional electrical field of a magnetospheric origin, which, in turn, is caused by the turning of B_Z. About one hour after this turning, it can penetrate from the magnetosphere into the plasmasphere. Such strong changes of the height of the F2 layer at B_Z turns could only be detected from topside-sounder satellite data. Ground-based sounding data indicated a much smaller change in the height of the F2 layer at B_Z turns, due to the strong recombination in the bottom part of the F2 layer. Large-scale internal gravity waves, arriving at equatorial latitudes from the auroral oval, cause an intensification of the equatorial anomaly in both the daytime and nighttime.

4. Space plasma physics

Since an ionospheric topside sounder is immersed in a plasma, the sounder pulse produces echoes from electrostatic waves, in addition to the electromagnetic echoes used to produce topside vertical electron-density profiles. These electrostatic-wave echoes, often termed resonances, result from waves that are returned after traveling short distances (hundreds to thousands of meters from the spacecraft).

Since the ionosphere is a magnetized plasma, they occur at frequencies near the harmonics of the ambient electron gyrofrequency and at the upper-hybrid frequency, in addition to the electron plasma frequency. The main characteristics of the electrostatic-wave echoes have been well explained in terms of the propagation of electron plasma waves, where ion motions are neglected. This approximation, however, cannot explain all of the observations. In particular, spur-like features are commonly observed on the electron resonances, as well as thin echo traces, both at delay times approximately corresponding to multiples of the proton gyroperiod. Ion motions must be included in order to explain such features.

The proton echoes are most often observed in the frequency region below the plasma frequency. *Horita and Chen* [*1995*], however, found proton echoes associated with resonances known as the f_Q resonances (observed at frequencies above the plasma frequency), when Alouette II was near the dip equator and the dip angle was less than about 8°. They found these echoes to be composed of two components, each with a delay time slightly greater than the calculated proton gyroperiod. *Muldrew* [*1998*] provided an explanation of the proton echoes observed below the plasma frequency in terms of a pulse that is simulated by ions which are modulated by the original sounder pulse. It is a plasma-memory process, similar to those used to explain other phenomena observed on topside ionograms, as well as in laboratory plasmas. The explanation involves propagating Bernstein waves, to explain the observed antenna-spin modulation of the proton echo-delay times.

The above discussion indicates that the sounder produces a direct perturbation on the ambient plasma particles. The bistatic HF sounder, carried on the OEDIPUS-C tethered rocket [*James and Rumbold, 1995b*; *Eliuk et al., 1995*], provided striking visual evidence of such sounder plasma perturbation. One of the OEDIPUS-C payloads carried the sounder transmitter and the other carried a synchronized receiver. The receiver payload also carried a video camera. It recorded brilliant luminosity around the transmitting antennas during thruster separation of the payloads, when the sounder was operating. These RF discharges were closely related to the detection (on both payloads) of electrons accelerated to keV energies [*Barnes et al., 1996*; *Eliuk et al., 1996*].

Baranets et al. [*1995*] investigated such sounder-accelerated particles, resulting from the topside sounder on COSMOS 1809. The charged-particle spectrometer detected sounder-accelerated particles at the antenna resonance, and at the electron gyrofrequency and its harmonics. The detection of the latter were found to be very sensitive to the orientation of the sounder transmitting antenna, relative to the direction of the Earth's magnetic field.

Benson [*1997*] provided additional observational evidence for such sounder plasma perturbation. Near-equatorial Alouette-II topside-sounder data were presented that indicated that field-aligned electron-density irregularities (FAI) were either produced or enhanced by the sounder pulse under certain ambient plasma

conditions, namely, when the ratio of the plasma frequency to the gyrofrequency was moderately large and near an integer. The evidence was the presence of Z-mode echoes just above the propagation cutoff under these conditions. It was argued that the echoes were either ducted in or scattered from the sounder-produced (or -enhanced) FAI, and that the sounder was more efficient at heating the plasma when the plasma-frequency-to-gyrofrequency ratio was near an integer value.

Several recent theoretical studies may be relevant to the above interpretation. *Osherovich et al.* [*1997*] investigated linear and nonlinear cylindrical oscillations of electrons in a magnetized plasma; the cylindrical geometry was considered to be appropriate for FAI. In the linear domain, they found two fundamental frequencies, corresponding to the cold plasma Z- and X-wave cutoff frequencies. These resonances increased in amplitude and narrowed in bandwidth when the plasma-frequency-to-gyrofrequency ratio was near an integer. *Zabotin et al.* [*1997*] simulated the scattering signatures of Z-mode waves on topside ionograms due to FAI. They reproduced Z-mode scattering signatures in the frequency range between the Z cutoff and the electron plasma frequency, as well as between the plasma frequency and the upper-hybrid frequency. They found that the results were not sensitive to the condition of the plasma-frequency-to-gyrofrequency ratio being near an integer. One of their conclusions was that any such sensitivity must be due to the generation of the FAI, rather than to the scattering from them. *Calvert* [*1995*] investigated Z-, O-, and X-mode ducted propagation in weak FAI, using the cold-plasma dispersion equation. He found that in high-density regions, the Z-mode ducting was the strongest, and it changed from trough ducting to crest ducting as the frequency increased past a value approximately midway between the Z cutoff and the plasma frequency.

5. Wave propagation

Unique wave-propagation experiments in space have become possible with the launch of the OEDIPUS-A and C tethered rockets. These were tethered payloads, which achieved a near-field-aligned orientation, with separation distances of approximately 1 km. The OEDIPUS-C conducting tether was cut near apogee, in order to study propagation both with and without a tether present. Prior to the tether cut, the conducting tether and the sheath region of depleted plasma surrounding it acted like a coaxial transmission line, allowing efficient propagation of sheath waves [*James and Balmain, 1995a*; *Barnes et al., 1996*; *Eliuk et al., 1996*]. After the tether cut, direct bistatic propagation experiments were performed that provided a clear in-situ demonstration of Faraday rotation [*James and Calvert, 1998*]. Fringes were observed in the received signal, corresponding to the rotation of the plane of linear electric-field polarization for the combined O- and X-wave modes. Similar fringes were observed for the combined O- and Z-wave modes. Fringes were also observed that were attributed to single-mode propagation. These were attributed to the dispersion characteristics of the whistler and Z-mode waves.

6. Natural wave emissions

Topside sounders are ideal for investigating natural wave emissions. This is because the electrostatic plasma resonances and the electromagnetic plasma wave cutoffs, stimulated by the sounder transmitter pulse, greatly enhance the reliability of wave-mode identification of the numerous waves of natural origin that are detected during the listening time interval, while the sounder receiver is being used for echo detection. In addition, the sounder's remote-measurement capability of determining electron-density contours enables inferences to be made about wave source regions below the satellite. Armed with this capability and previous ISIS-I observations, *Benson* [*1995*] took issue with some conclusions about auroral kilometric radiation (AKR) source regions, based on high-altitude Viking Langmuir-probe observations. It was claimed that AKR could not be generated in regions where the electron density increased to the point where the ratio of the electron plasma frequency to gyrofrequency exceeded 0.14. Earlier ISIS-I observations, based on sounder measurements of the low-altitude source region appropriate to the upper density limit, indicated that the AKR quenching region corresponded to a frequency ratio closer to 0.2. *Benson* [*1995*] indicated that the reason for the difference may be due to differences in other parameters important for the generation of AKR, and/or to the different solar conditions when the ISIS I and Viking measurements were made. The issue is important to the theory of AKR, and to inferences about Saturn's magnetic field based on the spectra of Saturn's kilometric radiation. *Hilgers* [*1995*] replied, stating that the ISIS-I results may have missed the narrow electron-density cavities seen by Viking, because of a more-limited horizontal resolution.

7. Practical applications

The applications of ionospheric data to radio-wave propagation are well known, and will not be discussed here. We would like to present some recent results, which are not well known to the community of radio scientists and geophysicists. They concern the effects of anomalous atmospheric electric fields that penetrate into the ionosphere [*Pulinets et al., 1998*]. These modification effects suggest the possibility of using a topside sounder to diagnose processes on the ground and in the atmosphere, such as radioactive-pollution emergencies resulting from atomic power plants, seismically active regions, and volcano-eruption effects.

7.1 Radioactive pollution

Among the sources of large amounts of radioactive products emitted from the Earth into the atmosphere, we should mention the three strongest: Windscale (Great Britain), 1957; Three-Mile Island (USA), 1979; and the greatest one, Chernobyl (USSR), 1986. The Interkosmos-19 satellite was active during the Three-Mile Island

emergency, and passed over the region several hours after the event on March 28, 1979. This event was the most serious commercial nuclear accident in US history, and eventually led to fundamental changes in the way nuclear power plants were operated and regulated. The accident itself progressed to the point where over 90% of the reactor core was damaged. It was shown that such a radioactive cloud creates a strong electric field (up to several kV/m) at lower heights in the atmosphere [*Boyarchuk et al., 1997b*]. Calculations by Pulinets *et al.* [*1998*] showed a strong vertical atmospheric-field effect within the ionosphere. They showed that a large, two-pole structure (positive and negative deviations of electron concentration) forms in the F layer. Such ionospheric modifications were detected over Three-Mile Island after the incident by the Interkosmos-19 topside sounder, as shown in Figure 3. These poles mark the greatest deviations from average conditions, and are shown with "|" and "+" signs in Figure 3. These positions are to be compared with the location of Three-Mile Island, shown with a star. Taking into account that the magnitude of the ionospheric effect depends on the electric-field strength, and on the size of the area occupied by the anomalous field on the ground, topside sounding could be an ideal technique for the remote detection of radioactive pollution.

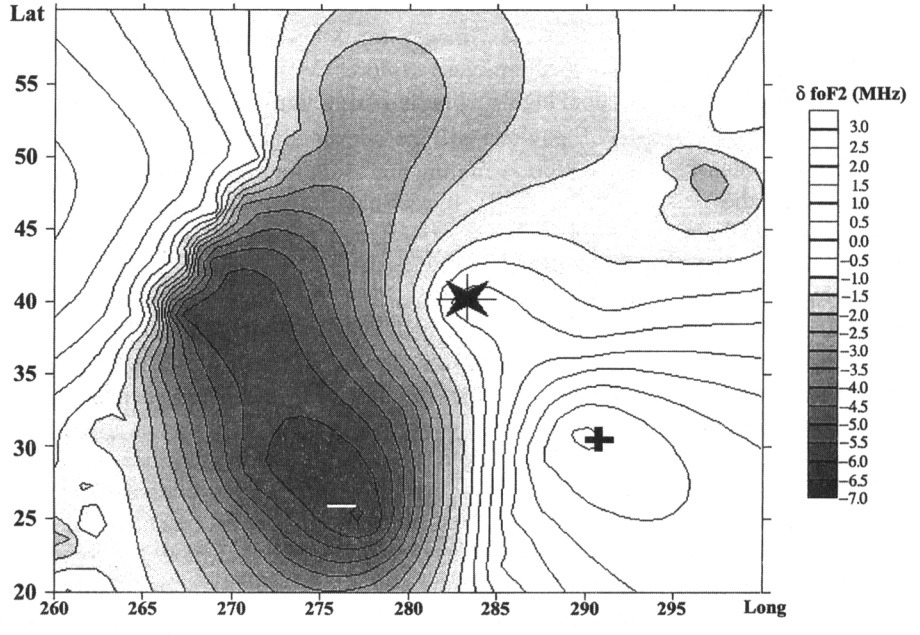

Figure 3. The deviation of the critical frequency in megahertz from the average level corresponding to undisturbed conditions, presented as a two-dimensional distribution (latitude-longitude) over the region of the Three-Mile Island atomic power plant, corresponding to a few hours after the emergency incident, as obtained from the Interkosmos-19 topside sounding data.

7.2. Seismic prediction

It was shown by *Boyarchuk et al.* [*1997a*] that an anomalous electric field could be generated due to radon emanation from the crust in seismically active regions after a series of ion-molecular reactions (the field was measured and found to exceed 1 kV/m). Therefore, the same two-pole structure (as discussed above, in connection with radioactive exhaust) could be formed within the ionosphere due to seismic activity. Such structures have been detected prior to strong earthquakes by topside sounders at various latitudes: Alaska (high latitudes), 1964: Alouette I [*Legen'ka, 1998*]; Central Italy (middle latitudes), 1980: Interkosmos-19 [*Pulinets and Legenka, 1997*]; New Guinea (equatorial latitude): Interkosmos-19 [*Pulinets et al., 1994; Biryukov et al., 1996; Pulinets, 1998*]. A multi-satellite system for short-term seismic prediction, based on topside-sounding measurements, has been proposed [*Pulinets, 1998*]. The same system could be used for global ecology monitoring, including radioactive pollution.

8. Magnetosphere and beyond

On January 1, 2000, IMAGE (Imager for Magnetopause-to-Aurora Global Exploration), the first NASA medium-class explorer (MIDEX) mission, is scheduled to be launched into an elliptical high-inclination orbit, with an apogee at a geocentric distance of $8R_E$. The IMAGE payload will include an advanced-design digital-radio sounder, capable of making direction-finding and Doppler measurements, and thus it is called a radio plasma imager (RPI). It will have capabilities similar to modern ground-based digital sounders [*Reinisch, 1996*]. Since IMAGE will spend most of its time in the electron-density cavity between the plasmapause and the magnetopause, the RPI will be able to obtain echoes from both the inward (from the plasmasphere) and outward (from the magnetopause region) directions. It will also get echoes from other boundaries, such as the cusp. The wide range of science objectives that will be addressed by the RPI has been discussed in a number of publications [*Calvert et al., 1995*; *Fung and Green, 1996*; *Green et al., 1996*; *Reiff et al., 1996*; *Benson et al., 1998*]. It will be possible to achieve these objectives despite the long distances to, and low electron densities of, some of the targets, because the RPI will employ long, crossed transmitting dipoles (each 500 m tip-to-tip) in the spin plane, and a 20 m tip-to-tip dipole along the spin axis, for reception. The RPI transmitting dipoles will also be used for reception. On-board signal-processing techniques will improve the signal-to-noise ratio. Not all agree that such measurements will be possible, and the claims made by the RPI team have generated some controversy in the scientific literature [*Greenwald, 1997a*; *Calvert et al., 1997*; *Greenwald, 1997b*].

On February 8, 1992, the first observations of a non-terrestrial magnetosphere by a relaxation sounder were made when the Ulysses spacecraft obtained a gravitational boost from Jupiter, on its way out of the ecliptic plane to fly over the

poles of the Sun. The sounder was part of the Unified Radio Plasma Wave (URAP) instrument. *Moncuquet et al.* [*1997*] interpreted the plasma resonances stimulated by the URAP relaxation sounder in terms of Doppler-shifted f_O resonances and Doppler-shifted electron gyro-harmonic resonances. They then determined the electron density as a point of comparison with electron densities deduced from their interpretation of the observed spectrum of quasi-thermal noise. They claimed good agreement between the two techniques, but failed to compare their results with previously published electron-density determinations (which yielded larger values), based on the same instrument during the same time interval, during this Io plasma torus encounter. *Benson et al.* [*1997*] supported the previously-published URAP-sounder electron-density determinations by arguing that the electron gyro-harmonic resonances were not observed in the Io plasma torus, due to the relatively long receiver dead time, and due to the inability to satisfy the echo rendezvous conditions.

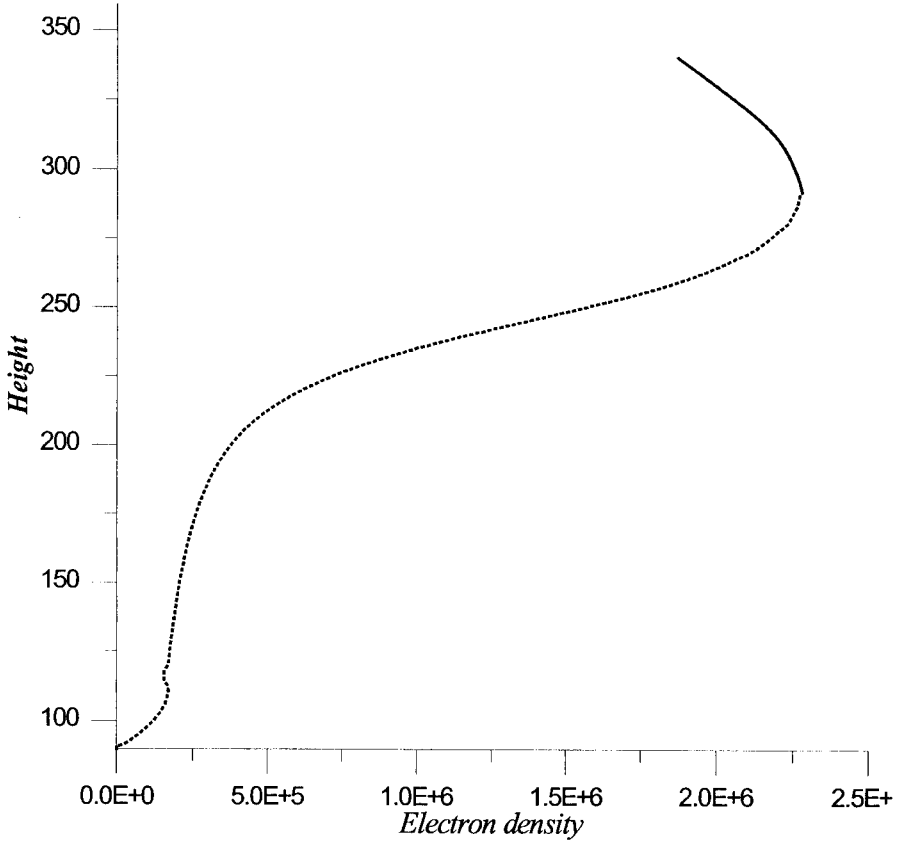

Figure 4. A topside–bottom-side profile of electron concentration (topside profile: bold line, bottom-side profile: dashed line), April 21 1999, 07-15 UT, Chung-Li, Taiwan, 24.9°N, 121.24°E.

Considering the scientific value of radio-frequency sounders in space, and the miniaturization of the instrumentation that has become possible with digital design, such sounders will most likely be proposed for future planetary missions. *Parrot et al.* [*1996*] discuss the scientific objectives that could be achieved with a sounder weighing less than 2 kg, a power consumption of less than 10 W, and a telemetry rate of 3 Mbits/day on the surface of Mars. They stress the need for such a sounder in order to understand the Martian solar-wind interaction, and its influence on the upper atmosphere of Mars.

9. Within and under the peak

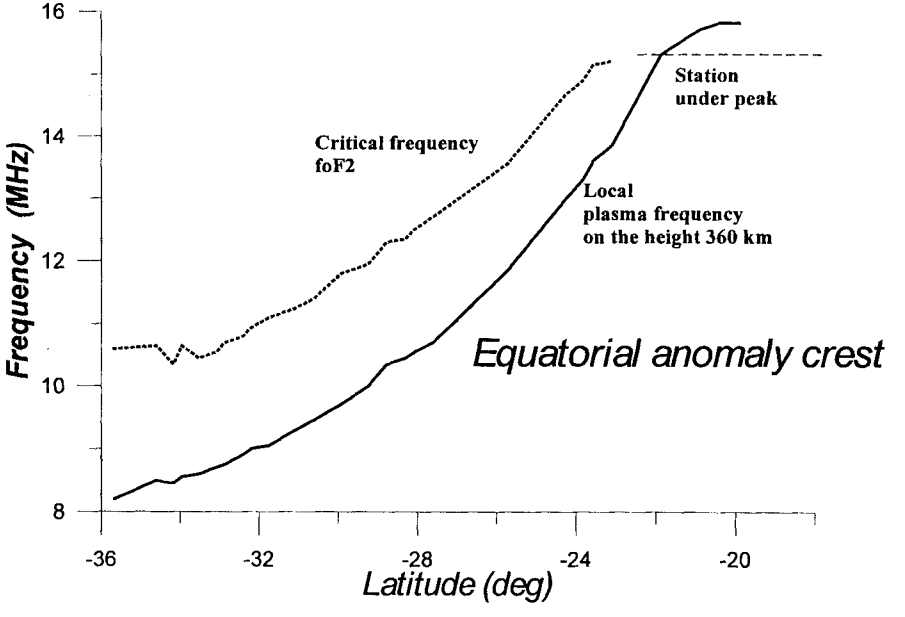

Figure 5. The equatorial anomaly crest parameters as a function of latitude while the MIR station was moving from north to south, from in situ measurements (bold line), and scaled critical frequency (dashed line).

After a lot of effort connected with malfunctions of the Russian MIR space station, the topside sounder (the replica of that from the Intercosmos-19 satellite) started normal operation onboard MIR at the end of 1998 [*www.orc.ru/~nickd*]. The low orbit of the MIR space station (~ 340 km) gives an unique opportunity to study in detail the peak height distribution, the detailed structure of the electron-density profile in the peak, wave propagation and plasma resonances within the peak and even under it, especially in equatorial regions in the equatorial anomaly crests. Figure 4 shows the combined vertical profile of the electron density while the MIR station passed nearby the Chung-Li ionospheric station (Taiwan, 24.9°N, 121.24°E). Simultaneous scaling of the local plasma frequency (the ordinary wave cutoff) and

the critical frequency in the vicinity of the crest demonstrates how the station enters under the peak of the density when the local plasma frequency and the critical frequency merge (See Figure 5). The unique reflection traces when the station is under the peak are now being processed. The experiment onboard the MIR space station is in preparation for the large program planned for the International Space Station topside sounder.

10. Summary

Ionospheric radio-frequency topside sounders have been well proven to be a versatile tool for investigating the ionosphere (on both an extremely local and a global scale), ionospheric wave phenomena, and ionospheric wave-particle interactions. The next century promises to extend this versatile capability into the terrestrial magnetosphere and beyond.

11. References

N. V. Baranets, V. A. Gladyshev and V. V. Afonin [1995], "Effect of HF Emission of the Topside Sounder Transmitter Aboard the COSMOS-1809 Satellite on the Ionospheric Plasma," *Adv. Space Res.*, **15**, pp. (12)95-(12)98.

G. Barnes, B. Gordon, H. G., and G. Rumbold [1996] "Transmitter/Receiver for OEDIPUS-C Ionospheric Wave Propagation Experiment," *Proceedings of the 9th Conference on Astronautics: "Toward the Next Century in Space,"* 13-15 November, Ottawa, Canada, Canadian Aeronautics and Space Institute, pp. 209-222.

R. F. Benson [1995], "Comment on 'The Auroral Radiating Plasma Cavities' by A. Hilgers," *Geophysical Research Letters*, **22**, pp. 3005-3007.

R. F. Benson [1996], "Ionospheric Investigations Using Digital Alouette/ISIS Topside Ionograms," in J. M. Goodman (ed.), *1996 Ionospheric Effects Symposium*, Alexandria, Virginia, pp. 202-209.

R. F. Benson [1997], "Evidence for the Stimulation of Field-Aligned Electron Density Irregularities on a Short Time Scale by Ionospheric Topside Sounders," *Journal of Atmospheric and Solar-Terrestrial Physics*, **59**, pp. 2281-2293.

R. F. Benson, J. Fainberg, R. A. Hess, V. A. Osherovich and R. G. Stone [1997], "An Explanation for the Absence of Sounder-Stimulated Gyroharmonic Resonances in the Io Plasma Torus by the Ulysses Relaxation Sounder," *Radio Science*, **32**, pp. 1127-1134.

R. F. Benson, B. W. Reinisch, J. L. Green, J.-L. Bougeret, W. Calvert, D. L. Carpenter, S. F. Fung, D. L. Gallagher, D. M. Haines, R. Manning, P. H. Reiff and

W. W. L. Taylor [1998], "Magnetospheric Radio Sounding on the IMAGE Mission," *Radio Science Bulletin*, **295**, pp. 9-20.

A. S. Biryukov, O. R. Grigoryan, S. N. Kuznetsov, V. N. Oraevsky, M. I. Panasyuk, S. A. Pulinets, V. M. Chmyrev [1996], "Space Physics and Ecology: Effects from the Earthquakes on the Ionospheric Heights" (in Russian), *Engineering Ecology*, **5**, pp. 92-115.

K. A. Boyarchuk, A. M. Lomonosov, and S. A. Pulinets [1997a], "Electrode Effect as an Earthquake Precursor," *Bulletin of the Russian Academy of Science. Physics, Physics of Vibration Quarterly Supplement*, New York, Allerton Press, **61**, pp. 175-179.

K. A. Boyarchuk, A. M. Lomonosov, S. A. Pulinets, and V.V. Hegai [1997b], "Impact of Radioactive Contamination on Electric Characteristics of the Atmosphere. New Remote Monitoring Technique," *Bulletin of the Russian Academy of Science. Physics, Physics of Vibration Quarterly Supplement*, New York, Allerton Press, **61**, 4, pp. 260-266.

W. Calvert [1995], "Wave Ducting in Different Wave Modes," *Journal of Geophysical Research*, **100**, 17, pp. 491-497.

W. Calvert, R. F. Benson, D. L. Carpenter, S. F. Fung, D. L. Gallagher, J. L. Green, D. M. Haines, P. H. Reiff, B. W. Reinisch, M. F. Smith and W. W. L. Taylor [1995], "The Feasibility of Radio Sounding in the Magnetosphere," *Radio Science*, **30**, pp. 1577-1595.

W. Calvert, R. F. Benson, D. L. Carpenter, S. F. Fung, D. L. Gallagher, J. L. Green, D. M. Haines, P. H. Reiff, B. W. Reinisch, M. F. Smith and W. W. L. Taylor [1997], "Reply," *Radio Science*, **32**, pp. 281-284.

N. P. Danilkin, G. M. Vaisman [1997], Positioning of the Satellite Ionosondes for the Global Ionosphere Monitoring, *Geomagnetism i Aeronomiya*, **37**, 1, pp. 191-196.

N. P. Danilkin, P. F. Denisenko, O. A. Maltseva [1998], "Peculiarities of Ionosphere Radiosounding from the Low-Altitude Satellites" *Geomagnetism i Aeronomiya*, **38**, 6, in press.

G. F. Deminova [1995a], "Wave-like Structure of the Longitudinal Variations of the Nighttime Equatorial Anomaly," *Geomagnetism i Aeronomiya*, **35**, 4, pp. 169-173.

G. F. Deminova [1995b], "Modifications in the Nighttime Low-Latitude Ionosphere After Southward Turning of the IMF," *Journal of Atmospheric and Terrestrial Physics*, **57**, 12. pp. 1459-1467.

P. F. Denisenko, E. V. Kuznetsov, N. V. Nastasyina and V. I. Vodolazkin [1998a], "Errors in Parameters Deduced from Ionospheric Soundings," in P. Wilkinson (ed.), *Computer Aided Processing of Ionograms and Ionosonde Records*, Report UAG-105, Boulder, Colorado, Published by WDC-A for Solar-Terrestrial Physics NGDC, pp. 76-81.

P. F. Denisenko, N. V. Nastasyina and V. V. Sotsky [1998b], "Using the Regularization Method for Electron Density Height Profile Reconstruction," in P. Wilkinson (ed.), *Computer Aided Processing of Ionograms and Ionosonde Records*, Report UAG-105, Boulder, Colorado, Published by WDC-A for Solar-Terrestrial Physics NGDC, pp. 82-87.

P. F. Denisenko, N. V. Nastasyina, V. V. Sotsky [1998c], "Application of the Regularization Method for Electron Density Height Profile Reconstruction by the Data of Vertical Topside Sounding," *Geomagnetism i Aeronomiya*, **38**, 1, pp.172-179.

A. K. Depueva and Y. Y. Ruzhin [1995], "Seismoionospheric Fountain-Effect as Analogue of Active Space Experiment," *Adv. Space Res.*, **15**, 12, pp. (12)151-(12)154.

W. Eliuk, R. Rob, G. Tyc, I. Walkty, G. Rumbold and H. G. James [1995], "Design of the OEDIPUS-C Suborbital Tethered Payload," *Proceedings of the Fourth International Conference on Tethers in Space*, 10-14 April, Hampton, Virginia, Science and Technology Corp., pp. 1749-1763.

W. Eliuk, I. Walkty, R. Rob, G. Rumbold and H. G. James [1996], "OEDIPUS-C Tethered Suborbital Mission Description and Flight Performance," *Proceedings of the 9th Conference on Astronautics: "Toward the Next Century in Space,"* 13-15 November, Ottawa, Canada, Canadian Aeronautics and Space Institute, pp. 332-341.

S. F. Fung, and J. L. Green [1996], "Global Imaging and Remote Sensing of the Magnetosphere," in *Radiation Belts: Models and Standards*, Geophysical Monograph 97, Washington, DC, American Geophysical Union, pp. 285-290.

J. L. Green, S. F. Fung and J. L. Burch [1996], "Application of Magnetospheric Imaging Techniques to Global Substorm Dynamics," in E. J. Rolfe and B. Kaldeich (eds.), *Proceedings of the Third International Conference on Substorms (ICS-3)*, Versailles, European Space Agency, ESA SP-389, pp. 655-661.

J. L. Green, W. W. L. Taylor, S. F. Fung, R. F. Benson, W. Calvert, B. Reinisch, D. Gallagher and P. Reiff [1998], "Radio Remote Sensing of Magnetospheric Plasmas," in R. F. Pfaff, J. E. Borovsky, and D. T. Young (eds.), *Measurements Techniques in Space Plasmas–Fields*, Geophysical Monograph 103, Washington, DC, American Geophysical Union, pp. 193-198.

R. A. Greenwald, [1997a], "Comment on 'The Feasibility of Radio Sounding in the Magnetosphere' by W. Calvert et al.," *Radio Science*, **32**, pp. 277-280.

R. A. Greenwald, [1997b], "Rebuttal to Reply by W. Calvert et al.," *Radio Science*, **32**, pp. 877-879.

T. L Gulyaeva., K. Barbatsi, J. Boska, G. de Francesci, S. S. Kouris, S. Moraitis, S. A. Pulinets, S. M. Radicella, I. Stanislawska, Th. Xenos, and M.-L. Zhang [1995], "Definition of Disturbance and Quietness with Topside Ionosonde Data," *Adv. Space Res.*, **16**, 1, pp.(1)43-(1)46.

A. E. Hedin, E. L. Fleming, A. H. Manson, F. J. Schmidlin, S. K. Avery, R. R. Clarke, S. J. Franke, G. J. Fraser, T. Tsuda, F. Vial, and R. A. Vincent [1996], "Empirical Wind Model for the Upper, Middle and Lower Atmosphere," *Journal of Atmospheric and Terrestrial Physics*, **58**, pp. 1421-1447.

A. Hilgers [1995], "Reply," *Geophysical Research Letters*, **22**, pp. 3009-3010.

R. E. Horita and G. M. Chen [1995], "Proton Cyclotron Echoes at the f_{Q3} Resonance," *Radio Science*, **30**, pp. 1569-1576.

Institute of Electrical and Electronic Engineers (IEEE) [1969], "Special Issue on Topside Sounding and the Ionosphere," *Proceedings of the IEEE*, **57**, pp. 859-1171.

N. I. Izhovkina, A. T. Karpachev, S. A. Pulinets [1996], "Structural Changes of a Upper Day Time Ionosphere on Data of the Interkosmos-19 Satellite," *Kosmischeskie Issledovaniya*, **34**, pp. 125-129.

J. E. Jackson [1969], "The Reduction of Topside Ionograms to Electron-Density Profiles," *Proceedings of the IEEE*, **57**, 6, pp. 960-976.

N. Jakowski [1996], "TEC Monitoring by Using Satellite Positioning Systems," in H. Kohl, R. Ruester, K. Schlegel (eds.), *Modern Ionospheric Science*, EGS Katlenburg-Lindau, pp. 371-390.

N. Jakowski and E. Sardon [1996], "Comparison of GPS-Derived TEC Data with Parameters Measured by Independent Ionospheric Probing Techniques," *Proceedings of the IGS Analysis Center Workshop*, March 19-21, Silver Spring, pp. 221-230.

H. G. James and K. G. Balmain [1995a], "Space Plasma Experiments with the Tethered OEDIPUS-C Payload," *Proceedings of the Fourth International Conference on Tethers in Space*, 10-14 April, Hampton, VA, Science and Technology Corp., pp. 1765-1779.

H. G. James and J. G. Rumbold [1995b], "The OEDIPUS-C Sounding Rocket Experiment," *Proceedings of the Fourth International Conference on Tethers in Space*, Washington, DC, 10-14 April, Hampton, VA, Science and Technology Corp., pp. 95-103.

H. G. James, and W. Calvert [1998], "Interference Fringes Detected by OEDIPUS C," *Radio Science*, **33**, pp. 617-629.

A. T. Karpachev [1995], "Distribution of Electron Concentration in the High Latitude Topside Ionosphere of a Southern Hemisphere for Nighttime Summer Conditions," *Geomagnetism i Aeronomiya*, **35**, 6, pp. 82-88.

A. T. Karpachev [1996], "Distribution of Electron Concentration Near F2 Layer Maximum in Northern Hemisphere for Nighttime Summer Conditions," *Geomagnetism i Aeronomiya*, **36**, 3, pp. 86-92.

A. T. Karpachev, G. F. Deminova, and S. A. Pulinets, [1995] "Ionospheric Changes in Response to IMF Variations," *Journal of Atmospheric and Terrestrial Physics*, **57**, 12, pp. 1415-1432.

A. T. Karpachev, M. G. Deminov, and V. V. Afonin [1996], "Model of the Mid-Latitude Ionospheric Trough on the Base of Cosmos-900 and Intercosmos-19 Satellites Data," *Adv. Space Res.* **18**, 6, pp. 221-230.

A. T. Karpachev, V. V. Afonin, J. Šmilauer [1997], "Distribution of the Electron Temperature in the Region of an Ionospheric Trough for Summer Nighttime Conditions," *Geomagnetism i Aeronomiya*, **37**, 1, pp. 96-102.

A. T. Karpachev, N. A. Gasilov, "Vertical Drift Variations with Longitude in the Midlatitude Nighttime Summer Ionosphere Calculated from H_mF2" [1998], *Geomagnetism i Aeronomiya*, **38**, 5, in press.

A. Kiraga, Z. Klos, H. Rothkaehl, Z. Zbyszynski, V. N. Oraevsky, S. A. Pulinets, I. S. Prutensky [1997], "Estimation of Electron Density of Ionospheric Plasma Using Wave, Impedance and Topside Sounder Data," *Adv. Space Res.*, **20**, 4/5, pp. 1083-1095.

A. D. Legen'ka [1998], private communication.

M. Moncuquet, N. Meyer-Vernet, S. Hoang, R. J. Forsyth and P. Canu [1997], "Detection of Bernstein Wave Forbidden Bands in the Jovian Magnetosphere: A New Way to Measure the Electron Density," *Journal of Geophysical Research*, **102**, pp. 2373-2379.

D. B. Muldrew [1998], "Topside-Sounder Proton-Cyclotron Echo Generation from a Plasma Memory Process and Electron Bernstein-Wave Propagation," *Radio Science*, **33**, pp. 1419-1435.

V. N. Oraevsky and S. A. Pulinets [1997], "Near-Real Time Monitoring of the Ionosphere From Space UNIGOAL-Space Weather Project Small-Satellite System," 8th Scientific Assembly of IAGA *Abstracts*, 4-15 August, Uppsala, Sweden, p. 381.

V. Osherovich, A. J. Fainberg, R. F. Benson and R. G. Stone [1997], "Theoretical Analysis of Resonance Conditions in Magnetized Plasmas When the Plasma/Gyro Frequency Ratio is Close to an Integer," *Journal of Atmospheric and Solar-Terrestrial Physics*, **59**, pp. 2361-2366.

M. Parrot, , J. G. Trotignon, J. L. Rauch, L. J. C. Wolliscroft, S. P. Kingsley, J. C. Cerisier, E. Blanc, C. D. Fry and R. J. Yowell [1996], "An Ionospheric Sounder for the Mars Landers," *Planet. Space Sci.*, **44**, pp. 1451-1455.

S. A. Pulinets [1989] "Prospects of Topside Sounding," in C. H. Liu (ed.), *WITS Handbook*, N2, Urbana, Illinois, SCOSTEP Publishing, Chapter 3, pp. 99-127.

S. A. Pulinets [1998], "Strong Earthquakes Prediction Possibility with the Help of Topside Sounding from Satellites," *Adv. Space Res.*, **21**, 3, pp. 455-458.

S. A. Pulinets and Z. Klos [1994], "The Possible Use of Solar Radiospectrometer SORS on the CORONAS Satellite for the Needs of PRIME," in *Proceedings of COST238/PRIME Workshop Numerical Mapping and Modelling and their Applications to PRIME*, Eindhoven, pp. 205-207.

S. A. Pulinets, A. D. Legen'ka, and V. A. Alekseev [1994], "Pre-Earthquakes Effects and their Possible Mechanisms," in H. Kikuchi (ed.), *Dusty and Dirty Plasmas, Noise and Chaos in Space and in the Laboratory*, New York, Plenum Publishing, pp. 545-557.

S. A. Pulinets, A. D. Legen'ka [1997], "First Simultaneous Observations of the Topside Density Variations and VLF Emissions before the Irpinia Earthquake, November, 23, 1980 in Magnetically Conjugated Regions," in M. Hayakawa (ed.), *Proceedings of International Workshop on Seismo Electromagnetics*, Chofu, Japan, University of Electro-Communications Publishing, pp. 56-59.

S. A. Pulinets, V. V. Hegai, K. A. Boyarchuk, A. M. Lomonosov [1998] "Atmospheric Electric Field as a Source of the Ionosphere Variability," *Uspekhi Fizicheskih Nauk*, **168**, 5, pp. 582-589; also in English in *Physics-Uspekhi*, **41**, 5, pp. 515-522.

P. H. Reiff, C. B. Boyle, J. L. Green, S. F. Fung, R. F. Benson, W. Calvert and W. W. L. Taylor [1996], "Radio Sounding of Multiscale Plasmas," in T. Chang and J. R. Jasperse (eds.), *Physics of Space Plasmas*, **14**, Cambridge, Massachusetts, MIT Center for Theoretical Geo/Cosmo Plasma Physics, pp. 415-429.

B. W. Reinisch [1996], "Modern Ionosondes," in H. Kohl, R. Ruster and K. Schlegel (eds.), *Modern Ionospheric Science*, Katlenburg-Lindau, Germany, European Geophysical Society, pp. 440-458.

N. A. Zabotin, D. S. Bratsun, S. A. Pulinets, and R. F. Benson [1997], "Response of Topside Radio Sounding Signals to Small-Scale Field Aligned Ionospheric Irregularities," *Journal of Atmospheric and Solar-Terrestrial Physics*, **59**, 17, pp. 2231-2246.